MINISTRY OF EDUCATION AND TRAINING

VIETNAM ACADEMY OF SCIENCE AND TECHNOLOGY

GRADUATE UNIVERSITY OF SCIENCE AND TECHNOLOGY

Nguyen Hai Anh

STUDY ON THE CONTROL OF NEGATIVE REFRACTIVE INDEX REGIONS BASED ON NEAR-FIELD INTERACTION EFFECTS IN METAMATERIALS COMBINED WITH EXTERNAL STIMULI

SUMMARY OF DOCTORAL DISSERTATION IN MATERIALS SCIENCE

Major: Electronic Materials

Code: 9 44 01 23

Ha Noi - 2025

Research Conducted at: Graduate University of Science and Technology, Vietnam Academy of Science and Technology

Supervisors:

1. 1st Supervisor: *Assoc. Prof. Dr. Nguyen Thi Hien, University of Sciences, Thai Nguyen University*
2. 2nd Supervisor: *Prof. Dr. Vu Dinh Lam, Graduate University of Science and Technology, Vietnam Academy of Science and Technology*

Referee 1: Assoc. Prof. Dr. Nguyen Hoang Nam

Referee 2: Assoc. Prof. Dr. Trinh Xuan Hoang

The dissertation will be defended before the Academy-level Dissertation Evaluation Council at the Graduate University of Science and Technology, Vietnam Academy of Science and Technology, at 9:00 a.m., December 22, 2025

The dissertation can be found at:

1. Library of the Graduate University of Science and Technology
2. National Library of Vietnam

INTRODUCTION

1. Rationale

Metamaterials (MMs) are artificially engineered materials in which the structural elements are arranged and controlled periodically (or sometimes aperiodically) to form unit cells that are much smaller than the operating wavelength. This unique structural arrangement enables metamaterials to exhibit electromagnetic properties that do not exist in natural materials or conventional composites.

Among various classes of metamaterials, negative refractive index metamaterials (NRI-MMs) represent one of the most remarkable research directions throughout the history of MM development. NRI-MMs possess the ability to fundamentally reverse the propagation of electromagnetic waves, allowing light to travel in a “backward” direction at an interface. This feature leads to extraordinary applications ranging from invisibility cloaking to perfect lenses that overcome the diffraction limit.

However, one of the major obstacles hindering the practical implementation of NRI-MMs is their narrow operational frequency bandwidth. The negative refractive index phenomenon strongly depends on the resonant response of the MM structure, resulting in a sharp resonance peak with a typical bandwidth of only about 5–10% of the central frequency. In addition to this bandwidth limitation, another significant challenge lies in the lack of active tunability of the negative permeability and refractive index after fabrication. To alter the operating frequency or the magnitude of the negative index, researchers often must redesign and refabricate the entire structure, which is costly and impractical for real applications. Efforts to broaden the operational bandwidth and achieve active control of NRI-MMs have faced several constraints, such as increased losses and reduced transmission efficiency. Consequently, most NRI-MM devices remain narrow-band, single-function, and passive. To address these challenges, researchers have discovered the near-field interaction effect, which occurs when resonant elements are placed in proximity, allowing their electric and magnetic fields to interact. This

interaction leads to the hybridization and splitting of the fundamental resonance modes, thereby generating new coupled resonances. Specifically, this mechanism—known as plasmon hybridization [13], [14], [15]—has become a powerful means to engineer broadband responses. However, the conventional approach still suffers from limited flexibility in dynamic control. By integrating smart functional materials, it becomes possible to externally tune the near-field interactions and thereby control the width, magnitude, and tunability of the negative-index and negative-permeability regions.

At the time of developing the doctoral dissertation proposal in 2022, the research direction focusing on expanding negative-index metamaterials through near-field interaction, as well as integrating external stimuli to control their operating frequency range, was attracting considerable interest from many research groups worldwide. Building on the research and development efforts of the Vietnamese research team and aligning with global trends, this dissertation will delve into the combination of hybridization methods and the control using external stimuli, thereby enabling the manipulation of the magnetic-negative and negative-index regions and addressing the aforementioned limitations.

2. Research Objectives

To select a material system with high flexibility (e.g., mechanical softness and externally tunable electromagnetic properties), easy integration, and low cost, with the aim of partially or fully replacing traditional components in metamaterials (MMs), particularly those in which magnetic-negative and negative-index regions are formed based on near-field interaction effects. The optimization of this material system focuses on tuning key operational parameters such as resonance frequency, bandwidth, response amplitude, and quality factor in the GHz/THz frequency range.

To clarify the physical mechanism of near-field interaction effects in the metamaterial system under the influence of external stimuli, thereby quantitatively evaluating the tunability of negative refractive index and

magnetic permeability. At the same time, to determine the influence of external factors (thermal, electrical) on frequency shifts, variations in response amplitude, and the ability to expand or narrow the negative-index region formed by near-field interactions in the GHz/THz range.

3. Research Scope and Content

The research focuses on controlling the magnetic-negative and negative-index regions of metamaterials through (i) Exploiting plasmon hybridization effects (first-order and second-order) to broaden the resonance band (ii) Integrating functional materials (graphene and VO_2) into the MM structure to enable active control via external stimuli (voltage and temperature) (iii) Investigating the mechanism of near-field coupling and the influence of dielectric losses and metallic conductivity (iv) Designing, simulating, fabricating, and characterizing MM structures operating in the GHz and THz frequency ranges.

4. Scientific and Practical Significance

Scientific significance: Clarify the physical mechanism of plasmonic hybridization and its tunability via external stimuli. Establish a theoretical framework for reconfigurable negative-index metamaterials.

Practical significance: Develop broadband, tunable MM structures operating in the 5G/6G frequency band (252–321 GHz, IEEE 802.15.3d-2017). Enable applications in telecommunication devices, reconfigurable antennas, sensors, and biomedical systems.

5. Novel Contributions

This dissertation focuses on addressing the problem of actively controlling and broadening the negative refractive index region of NRI-MMs through hybridization effects combined with external stimuli, encompassing the following key contributions:

(i) The dissertation clarifies the electromagnetic nature and control mechanism of electrically driven tuning based on graphene integration in first-order hybridized NRI-MMs operating in the THz frequency range. Two distinct structures were designed and demonstrated to (a) switch between negative-index transmission and reflection modes, and (b) achieve

continuous transition between positive-index and negative-index transmission by varying the Fermi level of graphene.

(ii) The dissertation elucidates the electromagnetic mechanism and thermal tuning behavior of VO_2-integrated NRI-MMs operating under first-order and second-order hybridization in the THz regime. The designed structures exhibit tunable magnetic-negative and negative-index regions, generating sharp, high-selectivity negative-index transmission peaks suitable for 6G frequency applications.

(iii) The dissertation successfully designed, fabricated, and experimentally characterized a second order hybridized magnetic- and negative-index metamaterial integrated with graphene conductive ink. The measured electromagnetic responses confirmed the interaction mechanisms and tunability predicted by theoretical and simulation models, validating the feasibility of the proposed designs.

Structure of the Dissertation

The dissertation consists of 145 pages, including an introduction, four main chapters, and a conclusion section.

CHAPTER 1. OVERVIEW OF NEGATIVE REFRACTIVE INDEX METAMATERIALS

1.1. General Introduction to Metamaterials

1.1.1. Historical Development of Metamaterials

The concept of materials with a negative refractive index was first proposed by the Russian theoretical physicist Victor Veselago in 1967 [8]. In his groundbreaking work, Veselago predicted the existence of materials exhibiting simultaneously negative permittivity (ε) and permeability (μ), which would result in a negative refractive index. According to his theory, such materials would display optical properties opposite to those of ordinary materials such as air or glass. Initially, Veselago's idea attracted little attention, primarily because no natural material was known to exhibit both negative ε and μ at the same time. Consequently, the concept remained theoretical for more than three decades. Building upon Veselago's theoretical foundation, John Pendry proposed artificial

structures capable of realizing these properties. In 2000, the research group led by David R. Smith at the University of California, San Diego (UCSD) successfully fabricated the first negative-index metamaterial [9]. Subsequent studies extended the field into various applications, such as Metamaterial Perfect Absorbers (MPA) [28] and Electromagnetically Induced Transparency (EIT) analogs in metamaterial systems, opening up new frontiers in electromagnetic manipulation.

1.1.2. Fundamental Principles in Metamaterial Research

The initial design framework of metamaterials is based on the Effective Medium Theory (EMT). When studying the interaction between electromagnetic radiation and matter, it is important to recognize that the wavelength of light is much larger than atomic dimensions and interatomic distances. Therefore, light cannot resolve individual atoms, allowing the material to be modeled as a homogeneous medium characterized by two macroscopic parameters: permittivity (ε) and permeability (μ).

In the Maxwell–Garnett model, the effective permittivity ε_{eff} of a medium consists of m spherical inclusions, each having a permittivity ε_i, embedded in a host medium with permittivity ε_m. When an electromagnetic wave interacts with a metamaterial, the energy is divided into three main components (neglecting diffraction and scattering): the reflected portion (R), arising from impedance mismatch; the absorbed portion (A), due to the intrinsic properties of the material; and the transmitted portion (T).

1.2. Overview of Negative Refractive Index Metamaterials

1.2.1. Materials with Negative Permittivity

In nature, metals exhibit negative permittivity only at frequencies below their plasma frequency. The permittivity ε of a metallic material depends on the incident electromagnetic frequency ω. However, at near-infrared and lower frequencies, the permittivity of metals becomes complex-valued, due to significant energy losses.

To achieve negative permittivity at lower frequencies (e.g., in the microwave regime), Pendry proposed a model of periodic thin metallic

wire arrays. These artificial structures effectively reduce the plasma frequency, thus enabling negative ε behavior in a frequency range much lower than that of bulk metals.

1.2.2. Materials with Negative Permeability

Most natural materials possess positive magnetic permeability, meaning that they can be magnetized in the presence of an external magnetic field. However, only a few materials exhibit negative magnetic permeability, i.e., they respond oppositely to an applied magnetic field. At low frequencies, such materials can still maintain magnetic behavior, but as the frequency increases to the GHz range, their magnetic properties are typically suppressed or vanish altogether.

Although not all materials are intrinsically magnetic like iron, nickel, or cobalt, magnetism can be artificially induced in non-magnetic materials by exciting circulating electric currents. When an electric current flows through a conducting loop, it generates a magnetic field surrounding the loop. If the loop is wounded into a coil, the magnetic field is concentrated at the center, forming a magnetic dipole moment. This phenomenon is known as magnetic induction. Based on this principle, several artificial structures capable of generating negative magnetic permeability have been proposed, most notably the Cut-Wire Pair (CWP) and Split-Ring Resonator (SRR).

1.2.3. Single-Negative and Double-Negative Metamaterials

To achieve a negative refractive index medium ($n' < 0$), the following conditions must be satisfied:

$$\mu'\varepsilon'' + \mu''\varepsilon' < 0. \tag{1.12}$$

Equation (1.12) indicates that the frequency regions exhibiting a negative refractive index can be classified into two types: single-negative (SN) and double-negative (DN) regions. In the double-negative region, both the real parts of permittivity and permeability (ε' and μ') are negative, while the imaginary parts (ε'', μ'') remain positive. In contrast, the single-negative region occurs when only one of the two quantities (ε' or μ') is

negative. In such a case, the imaginary parts (ε'', μ'') must be sufficiently large and positive to satisfy condition (1.12)

1.3. Hybridization Model and Mechanism for Broadening the Negative-Index Region

1.3.1. Theoretical Basis of Hybridization

In 2003, J. Halas and co-workers introduced a hybridization model to describe the plasmonic response of complex nanostructures [49]. Their study demonstrated that the resonant modes of a composite metallic nanosystem could be interpreted as the result of interaction (or hybridization) among the resonances of its constituent geometric elements. The hybridization theory provides a simple conceptual framework for designing nanostructures with tailored plasmonic resonances. The results of Halas et al. showed that the new hybridized plasmon resonance frequencies of a coupled system ($|\omega_+\rangle, |\omega_-\rangle, |\omega^+_{+,cs}\rangle$, $|\omega^-_{+,cs}\rangle$, $|\omega^+_{-,cs}\rangle$, $|\omega^-_{-,cs}\rangle$) arise from the splitting of the fundamental plasmon modes ($\omega_{sp} = \frac{\omega_B}{\sqrt{3}}$, $\omega_{sp} = \sqrt{\frac{2}{3}}\omega_B$, $\omega_{+,NS1}, \omega_{-,NS1}, \omega_{+,NS2}, \omega_{-,NS2}$) due to degeneracy lifting.

1.3.2. First-Order Hybridization Model

As mentioned earlier, the CWP structure is often regarded as a "magnetic atom", capable of generating negative magnetic permeability. In addition to magnetic resonance, CWP structures also exhibit electric resonances at different frequencies. The mode corresponding to a symmetric field distribution is termed the symmetric mode ($|\omega_+\rangle$), while the antisymmetric mode ($|\omega_-\rangle$) corresponds to an asymmetric field distribution. The antisymmetric mode ($|\omega_-\rangle$) is induced by an attractive interaction resulting from out-of-phase charge oscillations, leading to a lower energy level. In contrast, the symmetric mode ($|\omega_+\rangle$) arises from repulsive interactions caused by in-phase charge oscillations, thus corresponding to a higher-energy, higher-frequency resonance.

1.3.3. Higher-Order Hybridization Model

Similarly, in second-order and third-order hybridization, when previously hybridized elements interact with additional elements or with each other, more complex coupled resonance modes are formed, resulting in multi-level spectral splitting and enhanced tunability.

1.4. Controlling the Magnetic-Negative and Negative-Index Regions of Metamaterials via External Stimuli

The negative refractive index region is typically narrow and highly dependent on the polarization state of the incident electromagnetic wave. Controlling the refractive-index characteristics essentially involves tuning both the permeability (μ) and permittivity (ε) of the metamaterial. Therefore, one of the most actively explored approaches is to employ external stimuli—such as thermal, electrical, optical, or magnetic fields—to dynamically modify the electromagnetic properties of metamaterials, thereby enabling the tuning of resonance frequencies as desired.

1.4.1. Thermal Control of the Magnetic-Negative and Negative-Index Regions

When temperature increases, VO_2 undergoes a phase transition from an insulating to a metallic state, accompanied by a rise in electrical conductivity. This transition effectively short-circuits the gaps in SRR structures, gradually suppressing their magnetic resonance capability. In the case of InSb, as temperature rises, the carrier density (N) increases according to an empirical relation. The increased carrier density reduces the kinetic inductance (L_{mk}) of the structure, expressed as: $L_{\mathrm{mk}} = \frac{\pi m^*}{2t_{\mathrm{m}}Ne^2}$ where $m^*$is the effective mass, $t_m$is the film thickness, and $e$is the electron charge. The reduction in kinetic inductance shifts the fundamental magnetic resonance to higher frequencies and enhances the second-order hybridization between magnetic resonance modes.

1.4.2. Electric-Field Control of the Magnetic-Negative and Negative-Index Regions

Besides thermal tuning, the negative-index region can also be controlled by electrical or magnetic stimuli when combined with liquid-

crystal-based metamaterials. By applying an external electric or magnetic field to MMs incorporating anisotropic liquid crystals, one can modulate the permittivity and permeability of the composite medium, thereby dynamically altering its electromagnetic response and tuning the negative-index behavior.

1.4.3. Magnetic-Field Control of the Magnetic-Negative and Negative-Index Regions

Like tuning the frequency region with negative magnetic permeability in split-ring resonators (SRRs) using external electric fields, this region can also be controlled by applying an external magnetic field, achieved by introducing ferromagnetic materials into the metamaterial structure.

1.4.4. Electric Control of the Magnetic-Negative and Negative-Index Regions

The study by Xia Zhang et al. [64] demonstrated the active tunability of negative refractive index through the application of an external electric potential on graphene. The key breakthrough of this work lies in its ability to dynamically control the negative refractive properties of the metamaterial simply by adjusting the applied voltage across the graphene layer.

CHAPTER 2. RESEARCH METHODS

2.1. Theoretical Research Methods

2.1.1. Simulation Method

The simulation approach using CST Studio Suite provides detailed insight into the interaction between metamaterials (MMs) and electromagnetic waves, which is often difficult to observe or experimentally. CST allows for visualization of the electric and magnetic field distributions around the structure, thereby clarifying the interaction mechanisms and wave absorption processes. Moreover, it enables the determination of surface current distributions, which are essential for analyzing the resonant nature of the structure.

2.1.2. Computational Method

In 1970, the Nicholson–Ross–Weir (NRW) method was introduced to calculate complex material parameters—such as refractive index, permittivity, permeability, and impedance—based on reflection and transmission data. Later, in 2004, X. Chen et al. [73] proposed an improved retrieval method for metamaterials, enabling the determination of effective electromagnetic parameters (ε, μ, n, z) from scattering parameters (S_{11}, S_{21}) and phase information. In the study of metamaterials, the interaction between electromagnetic waves and structured media often leads to distinct resonance phenomena, where the material exhibits exotic properties.

2.2. Experimental Research Methods

2.2.1. Fabrication Method

To fabricate metamaterials—particularly NRI-MMs—operating in the GHz frequency range, photolithography is commonly employed. This technique operates on the principle of using light exposure to locally alter the properties of a photoresist layer coated on the substrate, thereby forming the desired pattern corresponding to the designed structure.

2.2.2. Measurement of Scattering Parameters

To analyze the electromagnetic characteristics of metamaterials—such as transmission and reflection spectra—measurements are performed using a Vector Network Analyzer (VNA) at the Institute of Materials Science, Vietnam Academy of Science and Technology (VAST).

CHAPTER 3. CONTROL OF THE ELECTROMAGNETIC PROPERTIES OF MAGNETIC-NEGATIVE AND NEGATIVE-INDEX METAMATERIALS BASED ON FIRST-ORDER HYBRIDIZATION

3.1. Numerical Determination of Electromagnetic Parameters for a Metal Disk-Array Metamaterial

To investigate and control the magnetic-negative and negative-index regions, it is essential to accurately determine the effective electromagnetic parameters, including permittivity (ε), permeability (μ), refractive index (n), and impedance (z). In this dissertation, the retrieval method of Chen et al. was applied to compute these parameters using simulated transmission

(S_{21}), reflection (S_{11}), and phase data. A critical aspect of this process is identifying the correct branch index (m) in the refractive index equation to ensure continuity and accuracy of n across the frequency spectrum.

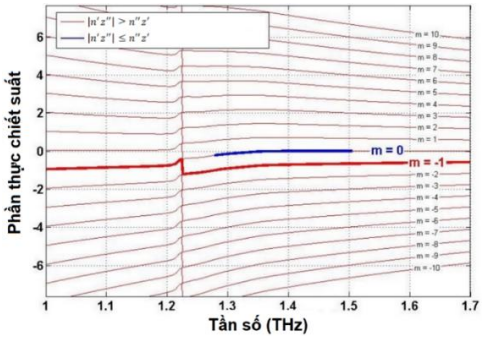

Figure 3.3. *Real part of the refractive index corresponds to different branches.*

3.2. Control of Magnetic-Negative and Negative-Index Properties in Graphene-Integrated First-Order Hybridized Metamaterials Operating in the THz Regime

3.2.1. Structural Design and Simulation

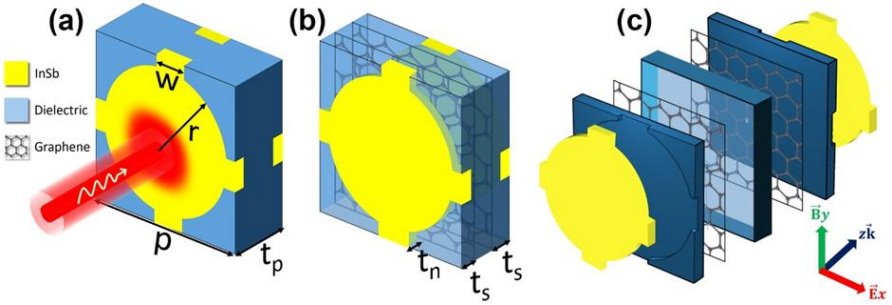

Figure 3.7. *(a) Unit cell of the metallic disk-array structure and its geometrical parameters; (b) Unit cell of the graphene-integrated metallic disk-array structure; (c) Constituent components of the graphene-integrated disk-array metamaterial.*

Figures 3.7(a) and 3.7(b) illustrate the unit cell of a graphene-integrated metal disk-array structure exhibiting a negative refractive index. The metamaterial (MM) features a periodic grid of metallic disks connected by continuous metallic wires. The structure is realized using two semiconductor InSb disk-array layers functioning as the metallic

components. InSb is particularly suitable for tunable negative-index metamaterials, primarily because its carrier concentration can be flexibly controlled by temperature, making it an ideal material for THz applications.

3.2.2. Simulated Electromagnetic Characteristics

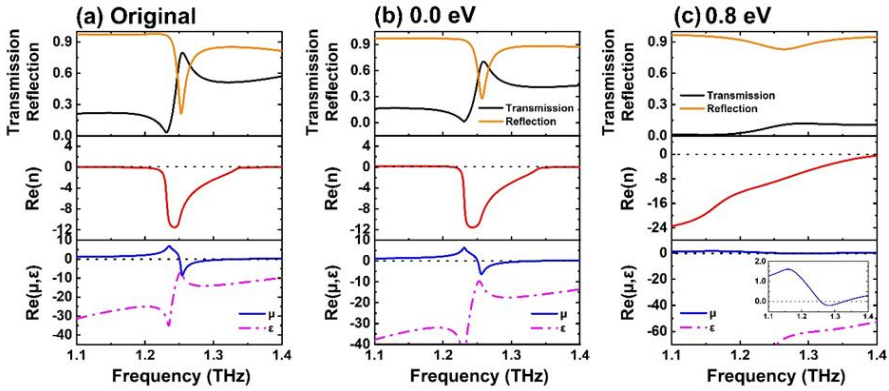

Figure 3.10. *Simulated transmission spectra and retrieved real parts of refractive index, permeability, and permittivity for (a) metal disk-array structure; (b) graphene-integrated disk-array structure at E_F = 0 eV; (c) graphene-integrated disk-array structure at E_F = 0.8 eV.*

The proposed metamaterial exhibits the ability to switch between transmission and reflection modes while maintaining a negative refractive index. The simulated transmission spectra and the real parts of refractive index, permeability, and permittivity for the graphene-integrated disk-array structure are shown in Figures 3.10(b) and 3.10(c) for two different Fermi energies: 0.0 eV and 0.8 eV, respectively. When a graphene sheet with Fermi energy = 0.0 eV [Fig. 3.10(b)] is added to the original design, the transmission coefficient in the negative-index region decreases from 0.80 to 0.70, indicating a reduction in the strength of the negative refractive behavior.

3.3. Control of the Electromagnetic Properties of Graphene-Based First-Order Hybridized Metamaterials Replacing Metallic Components

3.3.1. Structural Design and Simulation

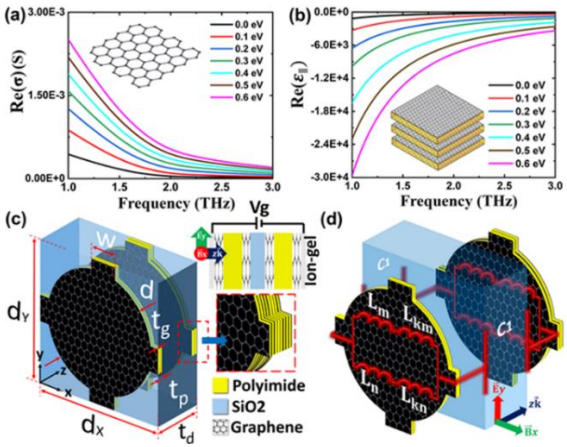

Figure 3.19. *(a) Real part of the surface conductivity of graphene for Fermi levels ranging from 0.0 eV to 0.6 eV; (b) Real part of the in-plane permittivity of the graphene composite; (c) Unit cell of the MMHGC structure with its geometrical parameters and constituent components; and (d) Equivalent LC circuit model of the MMHGC.*

The graphene-integrated metamaterial structure (Metamaterial based on a Hyperbolic Graphene Composite, abbreviated as MMHGC) operates in the THz frequency range with the ability to actively switch between negative refractive index (NRI) and positive refractive index (PRI) across a broad frequency band. In this design, multilayer graphene functions directly as the metallic component. Figure 3.19(c) presents a three-dimensional representation of the unit cell of the proposed MMHGC structure. The design incorporates a bilayer graphene composite (GC) embedded within a dishnet configuration, exhibiting metallic-like characteristics [119]. All components are embedded in a dielectric matrix with parameters $\varepsilon_d = 3.9$ and $\mu_d = 1.0$, forming a multilayer composite–composite sandwich structure.

3.2.2. Simulated Electromagnetic Characteristics of the Metamaterial

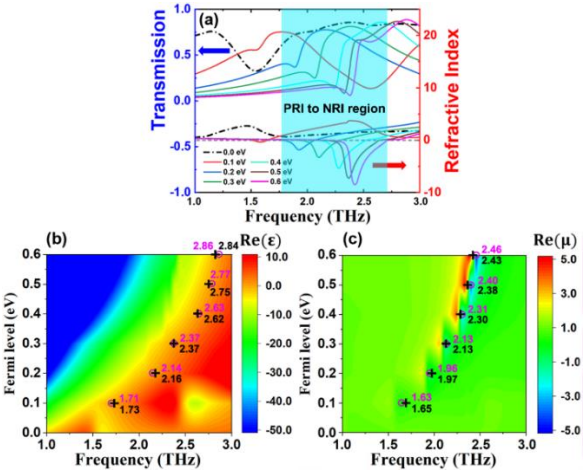

Figure 3.20. *Figure 3.20 illustrates the simulated electromagnetic response of the MMHGC: (a) Transmission spectrum and real part of the refractive index [Re(n)] at different Fermi levels; (b) Real part of the permittivity ε'; and (c) Real part of the permeability μ' corresponding to varying Fermi levels.*

When the Fermi level is 0.0 eV, the transmission band lies within the 1.0–3.0 THz frequency range. In this state, both the real parts of permeability (μ′) and permittivity (ε′) are positive, indicating a positive refractive index (PRI) response of the material. When the Fermi level is increased to 0.1 eV, the original transmission peak shifts into the negative region at 1.59 THz, as reflected by the drop of Re(n) below zero. Increasing the Fermi level further from 0.2 eV to 0.6 eV continues to modify the transmission spectrum, clearly revealing negative-index (NRI) behavior. Moreover, as observed in Figures 3.20(b) and 3.20(c), at higher Fermi levels, the transmission peak shifts toward higher frequencies, consistent with the overall trends in the real parts of n, ε, and μ. This confirms that the chemical potential of graphene serves as an efficient tuning parameter for broadband refractive index control in the THz regime.

3.4. Control of the Electromagnetic Properties of VO_2-Integrated Metamaterials Based on First-Order Hybridization

3.4.1. Design and Simulation of the Metamaterial Structure

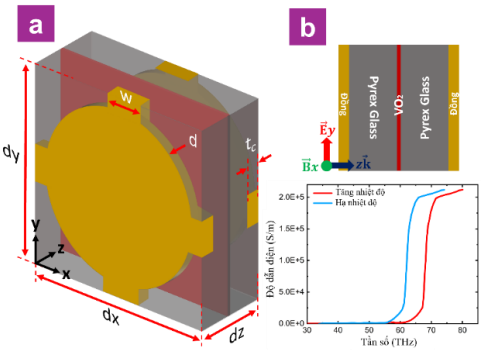

Figure 3.23. *(a) The disk-array metamaterial structure integrated with VO_2 and its optimized geometrical parameters; (b) The cross-sectional view of the structure and the temperature dependence of VO_2 conductivity, highlighting its insulator-to-metal transition.*

We present a VO_2-integrated negative-index metamaterial (NRI-MM) operating in the THz frequency range. The structure, illustrated in Figure 3.23(a), is designed as a metallic disk-array lattice, employing copper as the metallic element (conductivity = 5.96×10^7 S/m, thickness = 30 μm) deposited on a Pyrex glass substrate with a dielectric constant corresponding to a conductivity of 0.1448 S/m.

3.4.2. Simulated Electromagnetic Characteristics of the Metamaterial

Figure 3.24 depicts the significant variation in the electromagnetic response of the metamaterial structure as the VO_2 layer undergoes the dielectric-to-metallic phase transition. The transmission spectra shown in Figure 3.24(a) demonstrate a remarkable stability of the negative-index transmission band, maintaining a transmission amplitude of ~70% at 0.293 THz throughout the entire phase transition of VO_2. This stability contrasts

sharply with the pronounced suppression observed in the positive-index transmission (PRI) region at higher frequencies, where the transmission peak drops from above 90% to nearly zero. The asymmetric response between these two transmission bands enables the metamaterial structure to exhibit strong frequency selectivity within the double-negative (D-NRI) region.

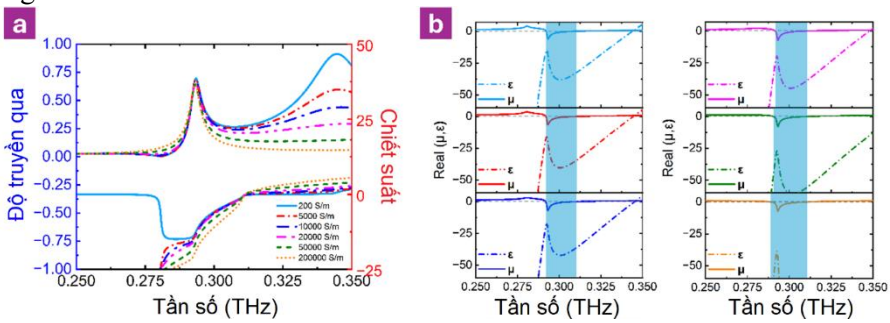

Figure 3.24. *Transmission spectrum, refractive index, and (b) effective parameters of the metamaterial, showing the double-negative region (D-NRI, blue) as a function of frequency for different VO_2 conductivities.*

The real part of the impedance, shown in *Figure 3.25(a)*, illustrates the evolution of impedance matching conditions as the VO_2 conductivity increases from 200 S/m to 200,000 S/m. A well-defined impedance matching region is observed around 0.293 THz, corresponding to the NRI transmission peak. Importantly, the impedance matching at this frequency remains stable and nearly unchanged throughout the entire phase transition, consistent with the persistent NRI peak behavior. In contrast, within the higher-frequency PRI region—particularly around the PRI transmission peak at 0.346 THz—significant impedance mismatch occurs: the structure transitions from well-matched at low conductivity to nearly unmatched (≈ 0) at high conductivity values. This loss of impedance matching at higher frequencies, combined with its preservation in the NRI region, explains the

mechanism underlying the frequency-selective transmission observed in Figure 3.24.

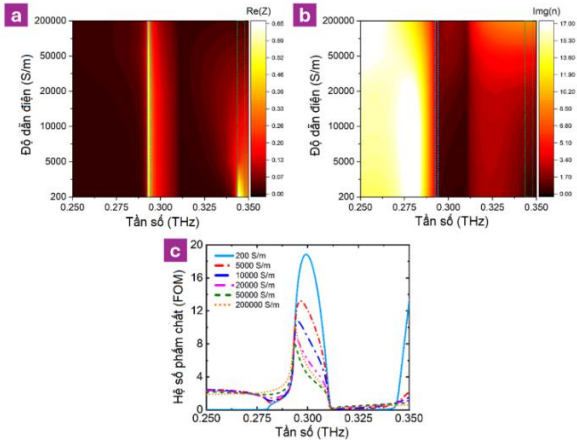

Figure 3.25. *(a) Real part of the impedance; (b) Imaginary part of the refractive index; and (c) Figure of Merit (FOM) of the metamaterial structure as a function of frequency for different conductivities of* VO_2

CHAPTER 4. CONTROL OF THE ELECTROMAGNETIC PROPERTIES OF MAGNETIC-NEGATIVE AND NEGATIVE-INDEX METAMATERIALS BASED ON SECOND-ORDER HYBRIDIZATION

4.1. Control of Magnetic-Negative and Negative-Index Characteristics of Graphene-Ink–Integrated Metamaterials Operating in the GHz Regime

4.1.1. Design and Simulation of the Metamaterial Structure

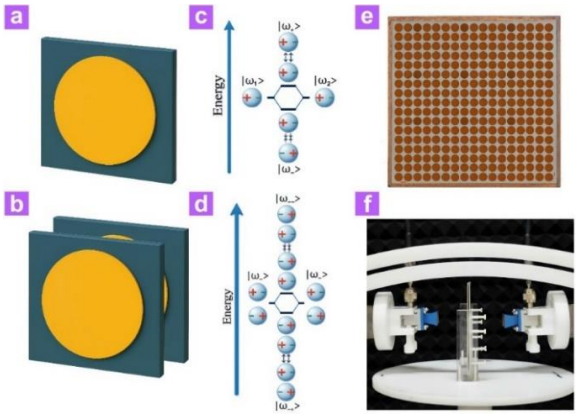

Figure 4.1. *(a) Unit cell of the single-layer dual-disk structure; (b) Unit cell of the double layer structure; (c) First-order hybridization diagram corresponding to the single-layer disk structure; (d) Second-order hybridization diagram corresponding to the double-layer disk structure; (e) Cross-section of the fabricated dual-disk sample; and (f) Experimental setup for transmission measurement.*

Figures 4.1(a) and 4.1(b) illustrate the unit cell of the dual-disk structure, corresponding to the single-layer and double-layer configurations, respectively. The dielectric substrate employed is Rogers RT6006. Figures 4.1(c) and 4.1(d) show the first order and second-order hybridization schematics corresponding to the single- and double-layer disk structures, respectively. Finally, the fabricated experimental sample and the transmission measurement setup are depicted in Figures 4.1(e) and 4.1(f). To realize the concept of tuning the transmission spectrum in the magnetic-negative region via hybridization, simulations and experimental measurements were conducted on samples coated with graphene conductive ink of different surface resistances, while keeping a constant layer thickness of t_{m1} = 0.035 mm, applied directly on the copper layer of the structure.

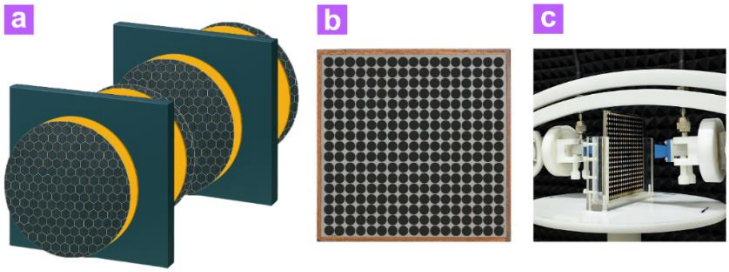

Figure 4.8. *(a) Unit cell; (b) Fabricated sample; and (c) Transmission measurement setup of the double-layer dual-disk structure integrated with graphene conductive ink.*

Figure 4.8(a) depicts the unit cell of a two-layer resonant system with an added conductive layer, maintaining the same design parameters and substrate (Rogers RT6006). The graphene layer fully covers the metallic surface, as illustrated in the figure. Figure 4.8(b) presents the fabricated sample coated with graphene, while Figure 4.8(c) shows the experimental setup used for transmission spectrum measurement.

4.1.2. Simulated Electromagnetic Characteristics of the Metamaterial

Figure 4.2(a) shows the simulated transmission spectra for the single- and double-layer configurations. The single-layer structure exhibits a narrow stopband at 14.36 GHz. In the double-layer configuration, this stopband broadens and splits into two distinct attenuation peaks at 14.101 GHz and 14.623 GHz, respectively. Figure 4.2(b) presents the corresponding experimental measurements, which show excellent agreement with the simulated results, thereby confirming the accuracy of the modeling approach. Figures 4.9(a) and 4.9(b) display the simulated and experimental transmission spectra, respectively, for two cases: (i) without graphene coating and (ii) with graphene conductive ink of surface resistance varying from 15 Ω/sq to 30 Ω/sq. In both cases, a consistent trend is observed — as the surface resistance increases, the non-

transmission region (corresponding to the magnetic-negative region) becomes narrower, and the signal attenuation decreases. Furthermore, the hybridization effect between the two layers effectively broadens the magnetic-negative region, confirming the expected coupling mechanism.

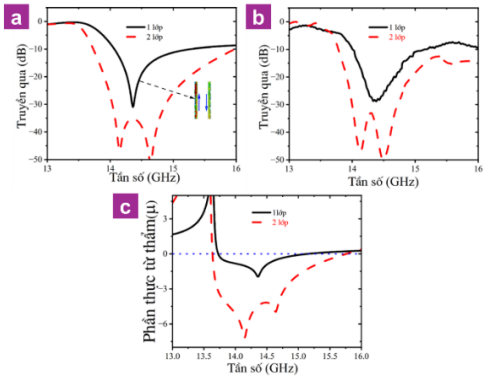

Figure 4.2. *Transmission spectra: (a) Simulated; (b) Measured; and (c) Calculated real part of the magnetic permeability for the single-layer/double-layer dual-disk structures.*

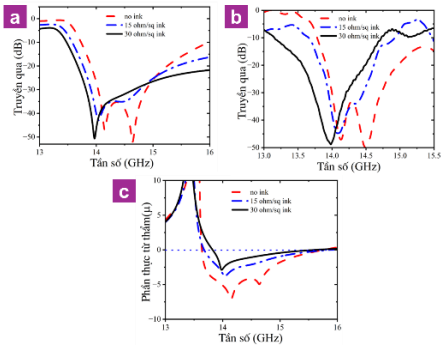

Figure 4.9. *Transmission spectra: (a) Simulated; (b) Measured; and (c) Calculated magnetic permeability of the double-layer dual-disk structures without and with graphene conductive coating of varying surface resistances.*

After analyzing the paired-disk structure exhibiting magnetic negativity, the dissertation further investigates the tunability of the

negative-index region through the hybridization mechanism by examining a metallic disk-array structure. The graphene ink layers were applied directly on the copper surface of the array. Figures 4.12(a) and 4.12(b) show the fabricated samples for the uncoated and graphene-coated cases, while Figures 4.12(c) and 4.12(d) present the simulated and experimental transmission spectra, respectively. The results demonstrate a high level of consistency between simulation and experiment. Notably, the attenuation at the second transmission peak (14.98 GHz) is significantly stronger than that at the first peak (14.63 GHz), indicating selective spectral suppression.

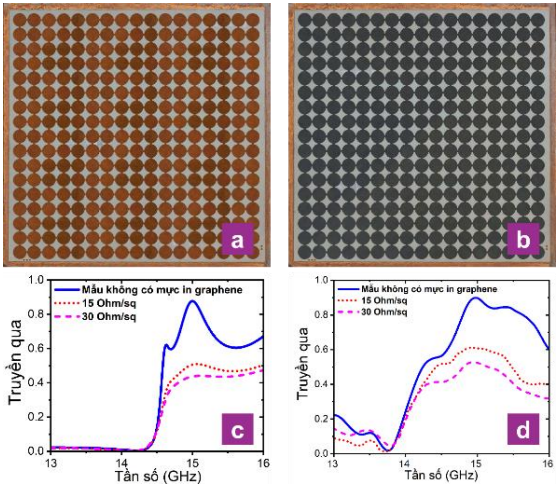

Figure 4.12. *(a) Unit cell of the metal disk-array structure without graphene coating; (b) Unit cell with graphene-ink coating; (c) Simulated transmission spectra; and (d) Measured transmission spectra of the uncoated and graphene-coated disk array structures with surface resistances of 15 Ω/sq and 30 Ω/sq, respectively.*

4.2. Control of Magnetic-Negative and Negative-Index Characteristics of VO_2-Integrated Second-Order Hybridized Metamaterials Operating in the THz Regime

4.2.1. Design and Simulation of the Metamaterial Structure

Transmission spectra: (a) Simulated; (b) Measured; and (c) Calculated magnetic permeability of the double-layer dual-disk structures with and without graphene conductive coating of different surface resistances. The proposed structure employs a second-order plasmonic hybridization mechanism between two disk-array dimers, separated by a Pyrex glass dielectric layer. Each dimer consists of a pair of copper disk arrays, symmetrically aligned through the dielectric substrate, as illustrated in Figure 4.14 [18]. The integration of vanadium dioxide in the intermediate Pyrex layer enables dynamic tunability via the metal–insulator phase transition (MIPT) of VO_2 with temperature variation [115], [132].

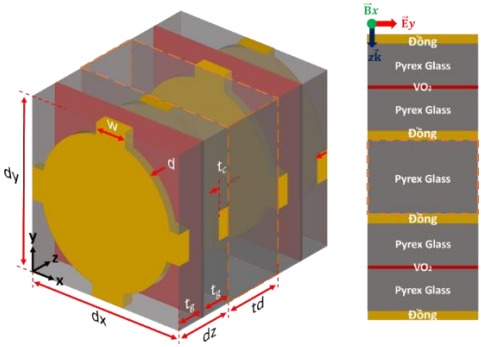

Figure 4.14. *Transmission spectra: (a) Simulated; (b) Measured; and (c) Calculated magnetic permeability of the double-layer dual-disk structures with and without graphene conductive coating of different surface resistances.*

4.2.2. Simulated Electromagnetic Characteristics of the Metamaterial

Figure 4.15(a) demonstrates the evolution of the transmission and refractive index spectra as the VO_2 conductivity increases from 200 S/m (insulating phase) to 200,000 S/m (metallic phase). The structure exhibits

two distinct negative-index peaks at 0.293 THz (D-NRI$_1$) and 0.2977 THz (D-NRI$_2$), along with a positive-index (PRI) peak at 0.3418 THz. *Figure 4.15(b)* shows that the transmission amplitudes of the three peaks respond differently as the VO_2 temperature (and thus conductivity) increases, confirming the active tunability of the system.

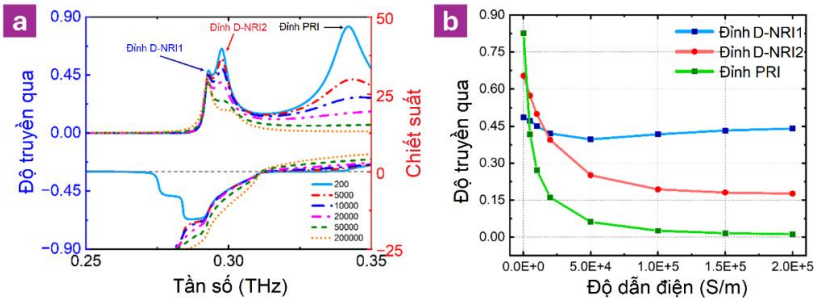

Figure 4.15. *(a) Transmission and refractive index spectra; and (b) Variation of transmission at the D-NRI and PRI peaks as a function of* VO_2 *conductivity.*

CONCLUSION

The dissertation "Study on the Control of Negative Refractive Index Regions Based on Near-Field Interaction Effects in Metamaterials Combined with External Stimuli" has successfully achieved its objectives, with the following main contributions:

1. First-Order Hybridization – Graphene Integrated within the Dielectric: Demonstrated active switching between negative-index transmission and reflection modes at 1.25 THz by varying the Fermi level from 0.0–1.0 eV. Transmission decreased from 0.70 to 0.12, while reflection increased from 0.28 to 0.83, maintaining stability within 300–400 K.

2. First-Order Hybridization – Graphene Replacing Metal (MMHGC): Achieved positive-to-negative index transition within 1.8–2.7 THz, with transmission amplitudes between 70–85%. The magnetic resonance

frequency shifted from 2.0 THz to 2.43 THz as the Fermi level increased from 0.2 to 0.6 eV.

3. First-Order Hybridization – VO_2 Integration: Maintained a stable NRI transmission peak (~70%) at 0.293 THz, while the positive-index peak was completely suppressed (from >90% to ~0%) as VO_2 conductivity varied from 200–200,000 S/m.

4. Second-Order Hybridization – Graphene Ink (GHz Regime): Successfully fabricated and measured a double-layer dual-disk structure.

5. Second-Order Hybridization – VO_2 (THz Regime): Observed three distinct resonances with different responses: D-NRI_1 remained stable, D NRI_2 decreased PRI peak was suppressed as VO_2 conductivity increased from 200 to 200,000 S/m.

Scientific Significance: The dissertation establishes a comprehensive physical basis for plasmon hybridization mechanisms and the role of functional materials in controlling and negative-index regions.

RECOMMENDATIONS FOR FUTURE RESEARCH

1. Investigate the influence of other external stimuli — such as pressure, magnetic fields, or optical excitation — on the negative-index region to explore more versatile tuning mechanisms.

2. Design metamaterial structures with broader bandwidths or higher quality factors, extending from the GHz to THz range.

3. Apply artificial intelligence and machine learning techniques for automated design and optimization of metamaterials with target electromagnetic properties.

4. Develop standardized measurement methodologies to accurately determine the effective electromagnetic parameters of fabricated negative-index metamaterials.

LIST OF PUBLICATIONS RELATED TO THE DISSERTATION

1. **Hai Anh Nguyen**, Bui Son Tung, Xuan Ca Nguyen, Vu Dinh Lam, Nguyen Thi Hien, Bui Xuan Khuyen, "*Tunable dynamic metamaterial for negative refraction*", Journal of Physics and Chemistry of Solids 186, 111804 (2024).

2. **Hai Anh Nguyen**, Thanh Son Pham, Bui Son Tung, Bui Xuan Khuyen, Dac Tuyen Le, Hai Yen Vu, Dinh Lam Vu, Nguyen Thi Hien "*Metamaterials based on hyperbolic-graphene composite: A pathway from positive to negative refractive index at terahertz*", Computational Materials Science 248, 113574 (2025).

3. **Hai Anh Nguyen**, Bui Xuan Khuyen, Bui Son Tung, Nguyen Thi Hien, Dinh Lam Vu, "*A comprehensive approach to retrieve effective properties in metamaterials*", Vietnam Journal of Science and Technology (2025) (ACCEPTED)

4. **Nguyễn Hải Anh**, Phạm Thanh Sơn, Bùi Xuân Khuyến, Bùi Sơn Tùng, Lê Đắc Tuyên, Phạm Minh Tân, Vũ Hải Yến, Lô Thị Huế, Vũ Đình Lãm, Nguyễn Thị Hiền , "*Phương pháp truy hồi đến kết quả tính toán các tham số trường điện từ của vật liệu biến hóa có chiết suất âm* ", 13th National Conference on Solid State Physics and Materials Science (SPMS 2023), 5-7/11, Ho Chi Minh city, Viet Nam, Vol 1, 263-268 (2023).